

# Migration of additives in polymer coatings: fluorinated additives and poly(vinylidene chloride)-based matrix

Bérengère Rixens, Romain Severac<sup>1</sup>, Bernard Boutevin\*, Patrick Lacroix-Desmazes

Laboratoire de Chimie Macromoléculaire, UMR 5076 CNRS-ENSCM, Ecole Nationale Supérieure de Chimie de Montpellier, 8, rue de l'Ecole Normale, 34296 Montpellier Cedex 5, France

Received 21 February 2005; received in revised form 15 March 2005; accepted 15 March 2005

## Abstract

In order to combine the properties of polymers based on vinylidene chloride (VC<sub>2</sub>) (barrier properties towards many gases) and fluorinated polymers (low surface energy, improvement of the chemical resistance), a diblock terpolymer poly(VC<sub>2</sub>-co-MA)-*b*-(PFDA) was synthesized by RAFT process. The first block is a statistical copolymer of vinylidene chloride (VC<sub>2</sub>) and methyl acrylate (MA) ( $M_n = 6800 \text{ g mol}^{-1}$  and PDI = 1.4), the second block is a homopolymer of 1H,1H,2H,2H-perfluorodecyl acrylate (FDA). The diblock terpolymer, when used in a coating formulation based on a poly(VC<sub>2</sub>-co-MA) matrix, migrates towards the surface of the coating and fluorinated moieties are located at the surface. The migration of the additive was clearly shown by scanning electron microscopy EDX and by measurements of surface energy, and the influence of the nature of the solvents used to prepare the coating was clearly established. These results indicate that the driving force for the migration is the surface energy of the additive.

© 2005 Elsevier Ltd. All rights reserved.

**Keywords:** Migration; Fluorinated diblock copolymer; Additive

## 1. Introduction

Additives for plastics and coatings are usually dispersed homogeneously within the bulk of the material. Such a distribution of the additives is interesting for plasticizers and various stabilizers (UV stabilizers, radical quenchers, etc...). However, in some other cases, it would be more interesting to get a preferential partitioning of the additives either at the surface (towards the air) or at the interface (towards the substrate of the coating). Preparation of this type of structure in only one step thanks to the use of smart additives which could migrate at the right place would represent an important technological progress. Several papers have studied the phenomenon of phase separation during the drying of the coatings, i.e. the so-called ‘self-

stratifying coatings’. The concept of ‘self-stratification’ has been introduced by Funke in 1976 [1]. His work deals with a powder mixture of two polymers deposited on a metallic surface. The polymers were separated into two layers upon heating. The self-stratification behavior was discussed in terms of solubility parameters and was related to capillarity phenomenon which depends on surface energy and viscosity [2]. These parameters were examined by several authors, all works being based on the study of a mixture of two incompatible polymers. Toussaint [3] has investigated the influence of the surface energy of several compounds and has shown that it is the compound with the lower surface energy which migrates towards the surface (air/coating interface). Vink [4] has estimated the degree of incompatibility between the phases by extension of the overlapping of spheres of solubility in the concept of Hansen’s solubility parameters [5]. Vink [4] has also used a mixture of two solvents (principle of preferential evaporation), one being a good solvent for the two resins and rapidly evaporating, the other being a good solvent for only one of the two resins and slowly evaporating. The first insoluble polymer comes into contact with the metal (coating/substrate interface). So, the mechanisms for self-stratifying coatings may be described in terms of solubility of blends, degree of incompatibility

\* Corresponding author. Tel.: +33 4 67 14 43 03; fax: +33 4 67 14 72 20.

E-mail address: [boutevin@cit.enscm.fr](mailto:boutevin@cit.enscm.fr) (B. Boutevin).

<sup>1</sup> Present address: Dupont de Nemours, route de chantereine, 78911 Mante-la-ville, France.

between the two phases, surface energy, and kinetics of evaporation of the solvents [6–8].

Fluorinated polymers have attracted interest as surface modifying agents because of their low surface energy [9, 10]. Works have shown that block copolymers containing a fluorinated block can efficiently partition towards the surface to form a surface separated domain [11,12]. Many kinds of block copolymers have been synthesized and the relation between the orientation of the fluorinated block and the surface properties has been studied [13]. The surface of the film can be characterized by atomic force microscopy (AFM) [13,14], surface energy measurement [14–16], X-ray photoelectron spectroscopy (XPS) [17,18]. Thus, fluoronomers, fluorinated oligomers and copolymers have been used to form thin films of fluorine-rich surface. The preparation and characterization of fluorine modified resin films have also been reported in many studies [18]. Furthermore, fluorinated surface modifying macromolecules (SMMs) were developed [16,19] and shown to reduce the hydrolytic degradation of base polyurethane. Mc Closkey et al. [16] have shown that fluorinated SMMs migrate to the surface of the SMM-poly(urethane urea) blends. Waltz et al. [20] have studied depth profiling of latex blend of fluorinated and fluorine-free acrylate with laser induced secondary mass spectrometry and showed a significant accumulation of fluorinated segments at the surface.

The aim of this study is to increase the surface properties of the coating with a small quantity of additive. Several parameters were important to induce a migration, like the molecular weight of the additive and its architecture. Indeed, the use of low molecular weight organic molecules as additives has shown some limitations. Low molecular weight additives can be leached off, as in the case of phthalates in poly(vinyl chloride), and high molecular weight additives can lead to a phase segregation and delaminating. The molecular weight of the additive should be tuned to permit its diffusion within the matrix while keeping a sufficient interaction with the matrix. Furthermore, an additive with a diblock structure appears to be attractive, one block ensuring the compatibility with the matrix while the other block brings the functionality and the driving force for the migration. A convenient method to control the molecular weight and the architecture of polymers is controlled/living radical polymerization (CRP) [21,22]. In this work, a matrix based on poly(vinylidene chloride) PVDC was prepared because this polymer is well-known for its barrier properties towards many gases [23,24]. Then, the fluorinated additive poly(vinylidene chloride-*co*-methyl acrylate)-*b*-poly(1H,1H,2H,2H-perfluorodecyl acrylate) was synthesized. It is a diblock copolymer containing two parts: one with the same composition as the matrix and the other one, which is fluorinated. The fluorinated block will generate the driving force for the migration of the additive. Finally, the additive was dispersed into the coating and its

migration was studied by two methods: surface energy measurements and scanning electronic microscopy.

## 2. Experimental part

### 2.1. Materials

Vinylidene chloride (VC<sub>2</sub>, Aldrich, 99%), methyl acrylate (MA, Aldrich, 99%) 1H,1H,2H,2H-perfluorodecyl acrylate (FDA, Aldrich) were purified by distillation under reduced pressure over CaH<sub>2</sub>. Benzene (SDS, 99.9%), methanol (SDS, 99.9%), dichloromethane (SDS, 99.9%), were used as received. Azobisisobutyronitrile (AIBN, Fluka, 98%) was recrystallized from methanol before use.

### 2.2. Equipment

Copolymerization was performed in a 300 mL stainless steel autoclave (Parr instrument) equipped with a pressure transducer, a temperature controller connected to an internal thermocouple inside the reactor, and with a tube to withdraw samples during the polymerization.

Suspension polymerization was performed in a 3 L vitrified autoclave with mechanical stirring, equipped with a temperature regulation and a pressure transducer.

### 2.3. Characterizations

Size exclusion chromatography (SEC) analyses were performed on crude samples with a Spectra Physics Instruments SP8810 pump equipped with two 300 mm columns PL-Gel 5  $\mu$ m mixed-C (polymer laboratories) and a Shodex Rise-61 refractometer detector. Tetrahydrofuran was used as eluent (1.0 mL min<sup>-1</sup>) at 30 °C. Molecular weights refer to a polystyrene calibration (polystyrene standards from polymer laboratories).

<sup>1</sup>H analyses were performed on a 200 MHz Bruker apparatus in CDCl<sub>3</sub> or THF D<sub>8</sub>. Tetramethylsilane (TMS) is used as an internal reference for <sup>1</sup>H NMR. Chemical shifts are given in ppm and assignments d, t, q, m stand for doublet, triplet, quadruplet and multiplet, respectively.

Thermal gravimetric analyses (TGA) were performed in nitrogen on a TGA 51 from TA instruments (Guyancourt, France) at a heating rate of 10 °C/min from 50 to 700 °C.

Differential scanning calorimetry (DSC) measurements were carried out using a Perkin–Elmer DSC Pyris 1 calibrated with indium. Each sample was scanned with a heating rate of 10 °C min<sup>-1</sup>. Four scans were performed on each sample. The measured DSC data are averaged on the three last subsequent scans.

Contact angles were determined with a Kruss G23 goniometer. The results are the average values of 15 measurements. Water (liquid surface energy  $\gamma_{LV} = 72.5$  mN m<sup>-1</sup>,  $\gamma_{LV}^D = 21.7$  mN m<sup>-1</sup>,  $\gamma_{LV}^P = 50.8$  mN m<sup>-1</sup>), hexadecane ( $\gamma_{LV} = \gamma_{LV}^D = 27.6$  mN m<sup>-1</sup>) and methylene

iodide ( $\gamma_{LV} = 49.4 \text{ mN m}^{-1}$ ,  $\gamma_{LV}^D = 48.1 \text{ mN m}^{-1}$ ,  $\gamma_{LV}^P = 1.3 \text{ mN m}^{-1}$ ) were used as wetting liquids. Metallic substrates were cleaned with acetone and dried. A polymer solution (concentration  $100 \text{ g L}^{-1}$ ) was spun-cast on the metallic plates (duration 30 s, acceleration 2000 rpm/s, spin rate 1000 rpm). Contact angle measurements were determined before and after annealing at  $110 \text{ }^\circ\text{C}$  during 7 h (temperature above the melting point of PFDA but below the degradation temperature of poly( $\text{VC}_2\text{-co-MA}$ )).

Two types of scanning electron microscopy (SEM) were used to determine the morphology of the coatings and the repartition of fluorine. Analyses were realized at the surface, at the interface, and in the bulk (cross section) of the coating material. Prior to analyses, samples were metallized with platinum, which is the more common method described.

SEM analyses were performed on a HITACHI apparatus (resolution, 5 nm) in order to study the morphology of the coating. The contrast of pictures depends on the molecular weight of each atom, low molecular weight elements appearing darker.

Scanning electronic microscopy coupled with X-ray SEM-EDX analyses were performed on a LEICA apparatus (resolution: 50 nm), in order to characterize the elements present in the sample. Characterization of every element (except hydrogen) was obtained by X-ray spectroscopy under electron flux. For this purpose, an electron beam is directed to the surface to be analyzed, and emitted X photons are detected. Thanks to the energy emitted by the elements, one can obtain an X-ray spectrum. Two types of analysis were performed. A whole analysis of the picture seen on the screen can be achieved, giving an average composition of the sample. Alternatively, a probe can be used to inspect surfaces within a  $1 \mu\text{m}^3$  scale, allowing studying the distribution of the different chemical elements in the cross section of the coating material by analyzing at different places.

EDX analyses were performed at the surface, at the interface and in the cross section of the coating. To compare the heights of the peaks, analyses were performed at the same magnification, the same electron beam tension (7 kV) and the same number of counts. To analyze the cross section of the coating, the sample was frozen in liquid nitrogen, then the coating was cryofractured and recovered with a scalpel.

#### 2.4. Synthesis of 1-(ethoxycarbonyl)eth-1-yl dithiobenzoate

The reversible chain transfer agent (CTA) was synthesized as already described [25,26]. The structure of this CTA is  $\text{PhC(S)SCH(CH}_3\text{)C(O)OEt}$ .  $^1\text{H NMR}$  in  $\text{CDCl}_3$   $\delta$ : 8.0 (d, 2H, Ph), 7.4 (m, 3H, Ph), 4.7 (q, 1H, SCH,  $^3J_{\text{HH}} = 7.46 \text{ Hz}$ ), 4.3 (q, 2H,  $\text{OCH}_2$ ,  $^3J_{\text{HH}} = 7.24 \text{ Hz}$ ), 1.7 (d, 3H,  $\text{SCH(CH}_3\text{)}$ ,  $^3J_{\text{HH}} = 7.46 \text{ Hz}$ ), 1.3 (t, 3H,  $\text{OCH}_2\text{CH}_3$ ,  $^3J_{\text{HH}} = 7.24 \text{ Hz}$ ).

#### 2.5. Preparation of the matrix component

Water (1400 g) were introduced in a 3 L autoclave. One hundred and ninety-two millilitres of a  $10 \text{ g L}^{-1}$  aqueous solution of a cellulosic dispersant were introduced in the autoclave under stirring at 350 rpm. AIBN (1.85 g,  $1.13 \times 10^{-2} \text{ mol}$ ) was then added. Oxygen was removed from the reactor by several vacuum/nitrogen cycles. Then, a mixture of vinylidene chloride (818 g, 8.44 mol) and methyl acrylate (181 g, 2.10 mol) was added. The autoclave was heated at  $70 \text{ }^\circ\text{C}$  for 18 h. Before opening the reactor, residual monomers were removed under vacuum for 1 h. A copolymer with molecular weight of  $M_n = 63,300 \text{ g mol}^{-1}$  and polydispersity index of  $\text{PDI} = 1.99$  was obtained with 92% yield (determined by gravimetry). Glass transition temperature  $T_g$  of this copolymer is  $32 \text{ }^\circ\text{C}$ .

#### 2.6. Synthesis of poly( $\text{VC}_2\text{-co-MA}$ ) by RAFT

The 300 mL autoclave was placed under vacuum. A solution of vinylidene chloride (65.8 g,  $6.79 \times 10^{-1} \text{ mol}$ ), methyl acrylate (15.13 g,  $1.76 \times 10^{-1} \text{ mol}$ ), AIBN (0.145 g,  $8.84 \times 10^{-4} \text{ mol}$ ) and CTA (1.35 g,  $5.33 \times 10^{-3} \text{ mol}$ ) in benzene (96.7 g, 1.24 mol) was introduced in the reactor under reduce pressure. Then, the autoclave was pressurized with 5 bars of nitrogen to allow withdrawing some samples during the polymerization. The reaction mixture was heated at  $70 \text{ }^\circ\text{C}$  and stirred at 400 rpm for 18 h. The conversion was determined by gravimetry as following: samples of about 2 g of the reaction mixture were withdrawn from the reactor tube and frozen in liquid nitrogen to stop the polymerization. Volatiles were evaporated under vacuum at  $35 \text{ }^\circ\text{C}$  (with hydroquinone to prevent polymerization). The global conversion in weight was calculated by  $(m_{\text{dry}} \times 100)/(m_{\text{sample}} \times \text{SC})$  where  $m_{\text{dry}}$  is the weight of the sample after evaporation,  $m_{\text{sample}}$  is the mass of the crude sample, and SC is the theoretical dry solid content at 100% conversion. The copolymer was dissolved in THF and purified by precipitation twice in pentane. The molecular weight was determined by SEC:  $M_n = 6800 \text{ g mol}^{-1}$ ,  $\text{PDI} = 1.4$ .

#### 2.7. Synthesis of poly( $\text{VC}_2\text{-co-MA}$ )-b-PFDA

Chain extension of the previous copolymer synthesized by RAFT was carried out as follows poly( $\text{VC}_2\text{-co-MA}$ ) (1.133 g,  $1.67 \times 10^{-4} \text{ mol}$ ), FDA (5.00 g,  $9.65 \times 10^{-3} \text{ mol}$ ), AIBN (0.0111 g,  $6.75 \times 10^{-5} \text{ mol}$ ) and benzene (24.57 g,  $3.15 \times 10^{-1} \text{ mol}$ ) were introduced in a schlenk. The mixture was deoxygenated by freeze thaw pump followed by a stream of argon. The mixture was heated at  $70 \text{ }^\circ\text{C}$  for 22 h. Then, the polymer was purified by precipitation twice in pentane and dried under vacuum.

## 2.8. Formulations and coating

Several formulations were prepared (Table 1) and coatings were realized by spin coating. The temperature chosen for annealing was 110 °C during 7 h (above  $T_m$  and  $T_g$ , 7 h to avoid degradation of the formulations).

## 3. Results and discussion

### 3.1. Diblock characterization

The diblock terpolymer was synthesized in two steps: first block synthesis of poly(VC<sub>2</sub>-co-MA) and then chain extension to produce poly(VC<sub>2</sub>-co-MA)-*b*-(PFDA). The first block was prepared by RAFT [27] polymerization (reversible addition–fragmentation chain transfer) in order to control the molecular weight of the copolymer. The incorporation of MA in the copolymer not only permits to make the polymer soluble in conventional solvents at room temperature but also increases its thermal stability [28]. The reactivity ratios of the monomers are close to 1 ( $r_1=0.90$ ;  $r_2=0.95$ ), it can be concluded that VC<sub>2</sub> gives an almost ideal statistical copolymer with MA [28]. The kinetic study shows that the molecular weight increases with conversion and the polydispersity index remains fairly narrow (Fig. 1(a)). Furthermore, the plot  $\ln([M_0]/[M])$  versus time is linear (Fig. 1(b)). These results are consistent with a good control of the polymerization.

After purification by precipitation, the isolated polymer ( $M_n=6800 \text{ g mol}^{-1}$ ,  $\text{PDI}=1.4$ ) has been reactivated for chain extension with 1H,1H,2H,2H-perfluorodecyl acrylate (FDA) by RAFT polymerization. PFDA has a very low solubility in usual organic solvents because of its high crystalline nature and its high fluorine content. Thus, the structural analyses of the fluorinated diblock terpolymer were difficult. Indeed, no common solvents were found for the two blocks. A first evidence of the diblock structure is the presence of foam both in THF (good solvent of poly(VC<sub>2</sub>-co-MA) but poor solvent of PFDA), and in trifluorotoluene (TFT) (good solvent of PFDA but poor solvent of Poly(VC<sub>2</sub>-co-MA)). This behavior can be attributed to the formation of micelles in THF (PFDA in the core of the micelles) and reverse micelles in TFT (poly(VC<sub>2</sub>-co-MA) in the core of the micelles) (Fig. 2). <sup>1</sup>H and <sup>19</sup>F NMR spectra in THF D<sub>8</sub> show the presence of

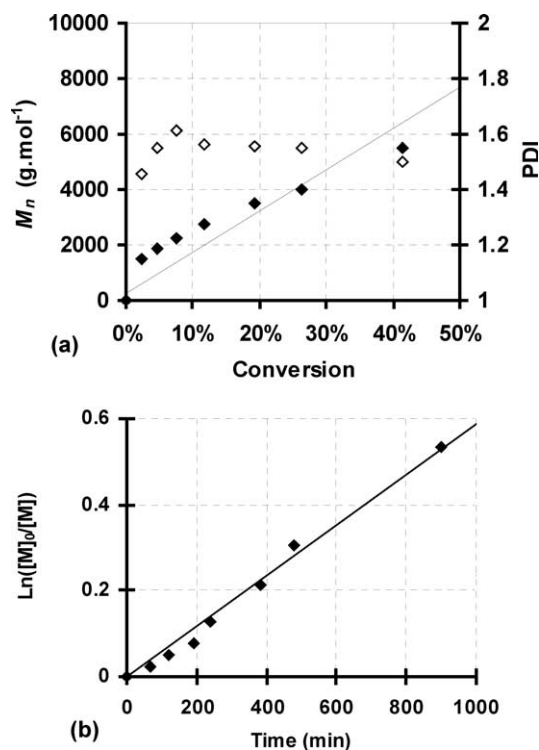


Fig. 1. Copolymerisation of VC<sub>2</sub> with MA by RAFT at 70 °C. (a) Evolution of molecular weight  $M_n$  (black symbols) and polydispersity index PDI (open symbols) versus conversion. (b) Evolution of  $\ln([M_0]/[M])$  versus time.

fluorinated units, but the length of the second block cannot be determined by <sup>1</sup>H NMR as this kind of analysis is not quantitative for micellar systems or aggregates.

Elemental analysis of poly(VC<sub>2</sub>-co-MA)-*b*-PFDA gives 30.37% C, 39.47% F, and 19.53% Cl. Thus the molar composition can be calculated 59% VC<sub>2</sub>, 15% MA, 26% FDA and a weight composition 28% VC<sub>2</sub>, 6.3% MA, 65.7% FDA (with  $M_{\text{VC}_2}=96.9$ ,  $M_{\text{MA}}=86.1$  and  $M_{\text{FDA}}=518 \text{ g mol}^{-1}$ ). Assuming that all the FDA units are in the diblock structure, the  $M_n$  of the terpolymer can be calculated by  $M_n=(100 \times 6800)/(28+6.3)=19,800 \text{ g mol}^{-1}$ . With the yield of polymerization (36%), the theoretical  $M_n$  calculated by  $M_{n,\text{th}}=m_{\text{FDA}}/n_{\text{CTA}} \times \text{conversion} + M_{\text{CTA}}$  is 17,700 g mol<sup>-1</sup>. The good correlation between these two  $M_n$  indicates that the average composition of the diblock terpolymer, according to the yield of polymerization, is poly(VC<sub>2</sub>-co-MA)<sub>57/15</sub>-*b*-(PFDA)<sub>21</sub>.

Table 1  
Weight composition of formulations for coatings

Formulation	Solvent	Matrix of poly(VC <sub>2</sub> -co-MA) ( $M_n=63,300 \text{ g mol}^{-1}$ , $\text{PDI}=1.99$ )	Additive poly(VC <sub>2</sub> -co-MA)- <i>b</i> -(PFDA)
a	THF	100%	–
b	THF	–	100%
c	TFT	–	100%
d	THF	84%	16%
e	THF/TFT(75/25 v/v)	91%	9%

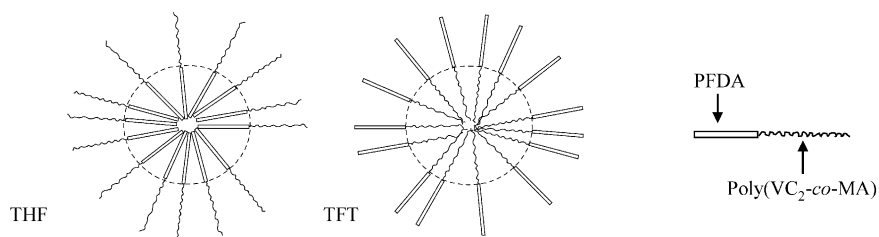


Fig. 2. Different structures of aggregates depending on the solvent: PFDA in the core in THF (left) or PFDA in the shell in TFT (right).

Poly(VC<sub>2</sub>-co-MA) copolymer, PFDA homopolymer and poly(VC<sub>2</sub>-co-MA)-*b*-PFDA diblock terpolymer were analyzed by thermogravimetric analysis (TGA) in order to check the presence of PFDA in the copolymer and to determine the temperature at which the diblock can be annealed without degradation (Fig. 3). Thermogravimetric analysis of the matrix shows a beginning of significant degradation at 200 °C, and two inflection points: one at 250 °C (HCl elimination) and the other at 510 °C. Analysis of the additive shows that it is stable below 200 °C. Two losses of weight were observed: the first one at 250 °C (degradation of the chlorinated block), the second one at 350 °C (degradation of the fluorinated block). Thermogravimetric analysis of PFDA homopolymer confirms the second weight loss (350 °C) corresponding to the fluorinated block.

DSC analysis of the fluorinated additive shows a  $T_g$  at 30 °C corresponding to poly(VC<sub>2</sub>-co-MA) and a melting point at 71 °C due to PFDA.

Solvent effect on the structure of the coating was studied. Two formulations (b and c) prepared with the block copolymer were analyzed (Table 1): one in THF (solvent of poly(VC<sub>2</sub>-co-MA) block), one in TFT (solvent of PFDA block). The coating obtained had a very low thickness (consequence of foam formation), thus only surface analysis were realized by microscopy after annealing at 110 °C. EDX spectra of the formulations b and c depict the presence of four elements of the terpolymers (C, F, O, Cl) and platinum used for metallization. The different peaks were attributed to carbon at 0.2 keV ( $K_{\alpha}$ ), oxygen at 0.05 keV ( $K_{\alpha}$ ), fluorine at 0.7 keV, the two peaks of chlorine at 2.6 ( $K_{\alpha}$ ) and 2.8 keV ( $K_{\beta}$ ), and the platinum peak at 2.1 keV (used for the metallization of the sample) (Fig. 4). The height of the fluorine peak implies that the additive contains a lot of

fluorine but it is not related to the molar ratio calculated by elemental analysis (39.47% F, and 19.53% Cl by elemental analysis, with  $M_F = 18.99$  and  $M_{Cl} = 35.45$  g mol<sup>-1</sup>, leading to a molar ratio F/Cl = 3.7). Moreover, the peak of fluorine is more important in TFT than in THF. This phenomenon can be explained by a different organization of the block copolymer depending on the solvent (Fig. 2). The results shown in Fig. 4 indicate that the thermodynamic equilibrium is not achieved for the coating. Nevertheless, our goal is not to use the additive alone but to put it in a formulation with the matrix. Furthermore, in practical applications, the thermodynamic equilibrium is not necessarily reached to obtain a migration of the additive during the curing of the coating.

### 3.2. Study of migration

The phenomenon of migration was studied by two techniques: contact angle measurements and microscopy (SEM and SEM-EDX).

#### 3.2.1. Surface energy measurement

Contact angle of a liquid on a film surface depends on the hydrophilicity/hydrophobicity of the surface. Polyacrylates such as PFDA are known to give low surface energy materials [29]. It was interesting to study the effect of the addition in various amounts of a PFDA block containing additive in a matrix of poly(VC<sub>2</sub>-co-MA) on the surface properties of dried films made from these mixtures, and in particular on their surface energy.

To determine the surface energy of the films, we used the technique based on the measurement of the contact angles  $\theta$

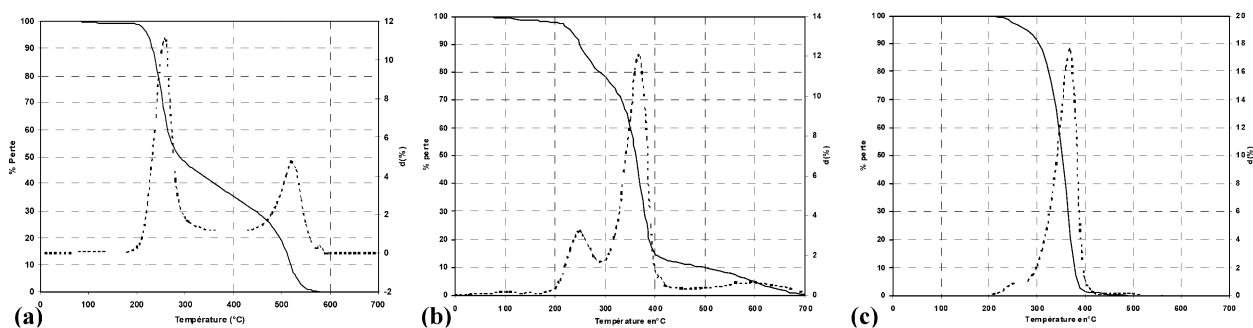


Fig. 3. Thermogravimetric analyses of polymers (a) poly(VC<sub>2</sub>-co-MA) matrix, (b) poly(VC<sub>2</sub>-co-MA)-*b*-PFDA additive, (c) homopolymer PFDA.

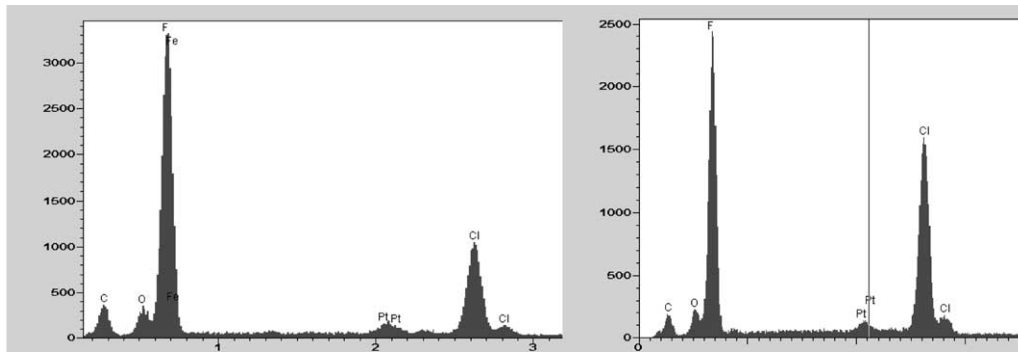


Fig. 4. Surface EDX analyses of coatings prepared from poly(V<sub>C2-co</sub>-MA)-*b*-PFDA in TFT (formulation **c**, left), and in THF (formulation **b**, right). (15 kV, × 700).

of very small drops of test liquids deposited onto a flat and smooth solid surface, here being the films.

The contact angle is related to the liquid used and the solid film surface energies, respectively noted  $\gamma_{LV}$  and  $\gamma_{SV}$ , through the well known Young's equation [30] (1):

$$\gamma_{SV} = \gamma_{SL} + \gamma_{LV} \cos \vartheta \quad (1)$$

where  $\gamma_{SL}$  is the surface interfacial (solid/liquid) energy.

According to the Fowkes' formalism [31], the surface energy ( $\gamma$ ) of a material can be decomposed in a (arithmetic) sum of two components, a dispersive and a polar one, respectively noted ( $\gamma^d$ ) and ( $\gamma^p$ ) such that:

$$\gamma_{LV} = \gamma_{LV}^d + \gamma_{LV}^p \quad (2)$$

$$\gamma_{SV} = \gamma_{SV}^d + \gamma_{SV}^p \quad (3)$$

Furthermore and among the various expressions for the interfacial surface energy which can be found in the literature (Kaelble [32], Owens and Wendt [33], Wu [34], van Oss [35]), we choose that one of Owens and Wendt for its simplicity [36]:

$$\gamma_{SL} = \gamma_{LV} + \gamma_{SV} - 2(\gamma_{SV}^d \gamma_{LV}^d)^{1/2} - 2(\gamma_{SV}^p \gamma_{LV}^p)^{1/2} \quad (4)$$

Combining (1) and (4), the Owens-Wendt/Young's equation [33] was obtained:

$$\begin{aligned} & \frac{\gamma_{LV}}{2(\gamma_{LV}^d)^{1/2}} (1 + \cos \vartheta) \\ &= (\gamma_{SV}^p)^{1/2} \left( \frac{\gamma_{LV}^p}{\gamma_{LV}^d} \right)^{1/2} + (\gamma_{SV}^d)^{1/2} \equiv ax + b \end{aligned} \quad (5)$$

which is the analytical expression for a straight line of slope  $a = (\gamma_{SV}^p)^{1/2}$  and y-axis intercept  $b = (\gamma_{SV}^d)^{1/2}$ .

Using different test liquids of known surface energies and for which their dispersive and polar components are also known, a set of different contact angle values are experimentally obtained. Plotting the values of  $(\gamma_{LV}/2(\gamma_{LV}^d)^{1/2})(1 + \cos \vartheta)$  versus  $(\gamma_{LV}^p/\gamma_{LV}^d)^{1/2}$  for each test liquids on a  $x, y$  diagramme allows the graphical determination of the slope  $(\gamma_{SV}^p)^{1/2}$  and the y-axis intercept  $(\gamma_{SV}^d)^{1/2}$  and hence the calculation of  $\gamma_{SV}$  through (3). The slope and the y-axis

intercept can also be determined more simply by the linear regression technique.

The experimental contact angles for the test liquids used in this study and the resultant surface energies of films we made from different mixtures polymer/additive are summarized in Table 2. Vink [4] has used a mixture of two solvents (principle of preferential evaporation) to induce the 'self stratification' in a blend of two polymers. Herein, a mixture of two solvents was also studied. THF is a good solvent for the matrix and for the block poly(V<sub>C2-co</sub>-MA) of the additive while TFT is a good solvent of the fluorinated block. Moreover, the boiling point of THF (65 °C) is below the one of TFT (100 °C) and should make the migration easier.

Results (Table 2) show the effect of the additive on the surface properties of the coating. The surface energy of the matrix agrees well with values reported for PVDC (40.0 mN/m), and contact angle with water of 80° and with methylene iodide of 29° [37]. The value for PFDA is the same as that reported in the literature (10.9 mN/m) [38]. The low surface energy of additive/matrix mixture shows that the fluorinated additive is present at the surface of the coating. Formulation **e** with two solvents (TFT and THF) gives a lower  $\gamma$  than formulation **d**, indicating a higher efficiency of the migration of the additive when two solvents are used. These results are in agreement with Vink theory. Thus, the decrease of the surface energy proves that the surface is enriched in the fluorinated additive. The following section on analyses by microscopy permits to prove the migration of the additive towards the surface.

### 3.2.2. Analysis by scanning electronic microscopy

Two types of SEM were used to visualize the morphology of the coatings and the repartition of the fluorinated additive: Scanning electron microscopy (SEM) and scanning electron microscopy coupled with X-ray (SEM-EDX). To compare the heights of the peaks, the analyses were performed at the same magnification, the same tension for the electron beam (7 kV) and the same number of counts. To analyze the cross section of the coating, the sample was frozen in liquid nitrogen, then the

Table 2  
Contact angles in degree after annealing (110 °C, 7 h) and corresponding surface energy

Solvent	Metallic substrate	Matrix (formulation <b>a</b> )	Additive (formulation <b>b</b> )	Mixture (formulation <b>d</b> )	Mixture (formulation <b>e</b> )
Water	58.0	77.0	122.5	105.2	119.4
Hexadecane	13.0	17.2	76.0	68.8	78.8
Methylene iodide	39.8	31.5	93.3	80.7	83.8
$\gamma_{sv}$ (mN/m)	47.1	38.1	10.9	15.7	12.3

coating was cryofractured. First, the sample was characterized at the surface (top view), then at the interface (bottom view), and finally the cross section was characterized by successive analyses with the probe of the microscope.

Like for formulations **b** and **c**, EDX spectra of the formulation **d**, (formulation in THF, annealed at 110 °C) shows the presence of different elements (Fig. 5). The peaks of carbon at 0.2 keV ( $K_{\alpha}$ ), oxygen at 0.5 keV ( $K_{\alpha}$ ), fluorine at 0.7 keV ( $K_{\alpha}$ ), and the two peaks of chlorine at 2.6 ( $K_{\alpha}$ ) and 2.8 keV ( $K_{\beta}$ ) can be distinguished. The peak of platinum, used for metallization, is also observed at 2.1 keV. The analysis of the surface of the coating shows the presence of fluorine. But the surface is not homogeneous: aggregates or nodules are observed on the photograph. EDX analyses show that the content of fluorine increases when pointing the nodules. These results indicate that the additive is incompatible with the matrix, probably due to the poor solubility of the additive in THF.

Then the cross section of formulation **d** was studied (Fig. 6). EDX analyses show the repartition of the additive. Indeed the presence of fluorine is only observed at the surface (air/coating) and in the bulk but not at the interface (coating/metal). Nevertheless, the amount of fluorine at the surface is lower than in the bulk (middle of the cross section).

These analyses do not prove the migration of the additive towards the surface of the coating but they show the presence of the additive near the surface and not at the interface. Moreover, these results are in agreement with the surface energy measurements. Indeed the presence of fluorine at the surface leads to a decrease of the surface energy  $\gamma$ . Lastly, the cross section is not homogeneous: small nodules are observed.

### 3.2.3. Influence of a mixture of two solvents

The photographs of formulation **e** (with solvent mixture) show that the surface is smoother than for formulation **d**, and the cross section seems free of nodules. Thus, two solvents improve the solubility of the additive in the matrix. Moreover, EDX analysis shows the presence of fluorine at the surface of the coating. Cross section of the coating has also been characterized. The migration of the additive is proved by EDX spectra (Fig. 7). Indeed, a fluorine gradient in the cross section is observed: a higher peak of fluorine at the surface (air/coating) and no peak of fluorine at the interface (coating/metal). This result shows that the migration occurs favorably if a selective solvent of the PFDA block is used in conjunction with a solvent of the matrix.

## 4. Conclusion

A diblock terpolymer poly( $VC_2-co-MA$ )-*b*-PFDA was prepared by RAFT process and was used as a fluorinated additive in coating formulations based on a poly( $VC_2-co-MA$ ) matrix. The additive has a low surface energy as shown by contact angle measurement. It contains two parts: one is compatible with the matrix (same composition) while the other one is fluorinated (incompatible with the matrix) and affords a driving force for the migration. EDX analyses have shown that the additive migrates towards the surface of the coating. Thus, the presence of the additive into the coating efficiently increases the hydrophobicity of the surface, enhancing the surface properties of the coating. The results of this study are in agreement with those of Toussaint and Funke on incompatible polymer blends.

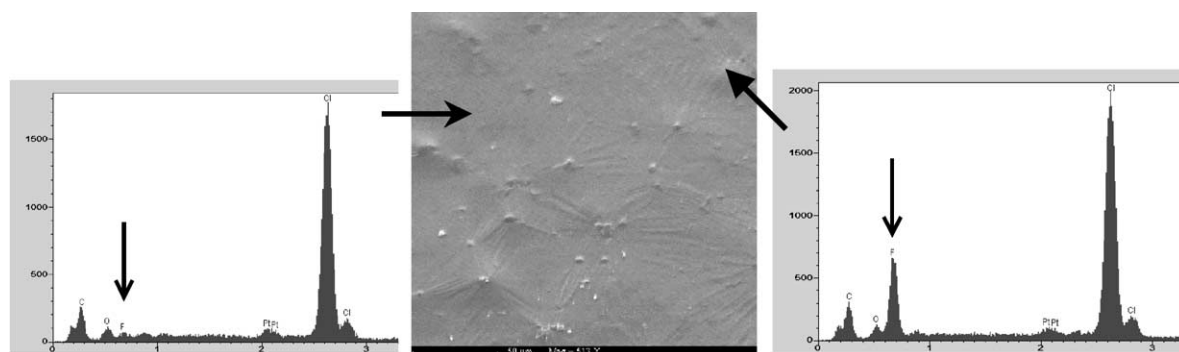


Fig. 5. EDX spectra of the surface (left), of a nodule (right) and photograph of the surface (middle), for formulation **d** in THF.

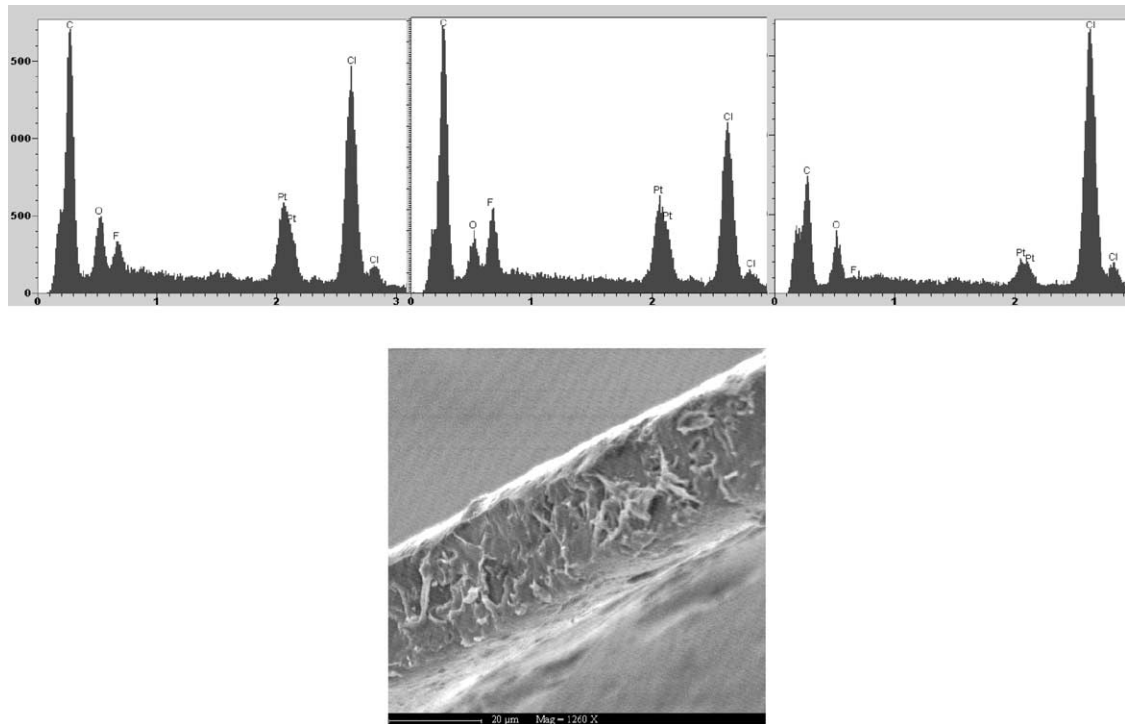


Fig. 6. EDX spectra of formulation **d** (after annealing at 110 °C) on the surface (left), in the middle of the cross section (center), interface (right), and SEM photograph of cross section of formulation **d** (after annealing at 110 °C).

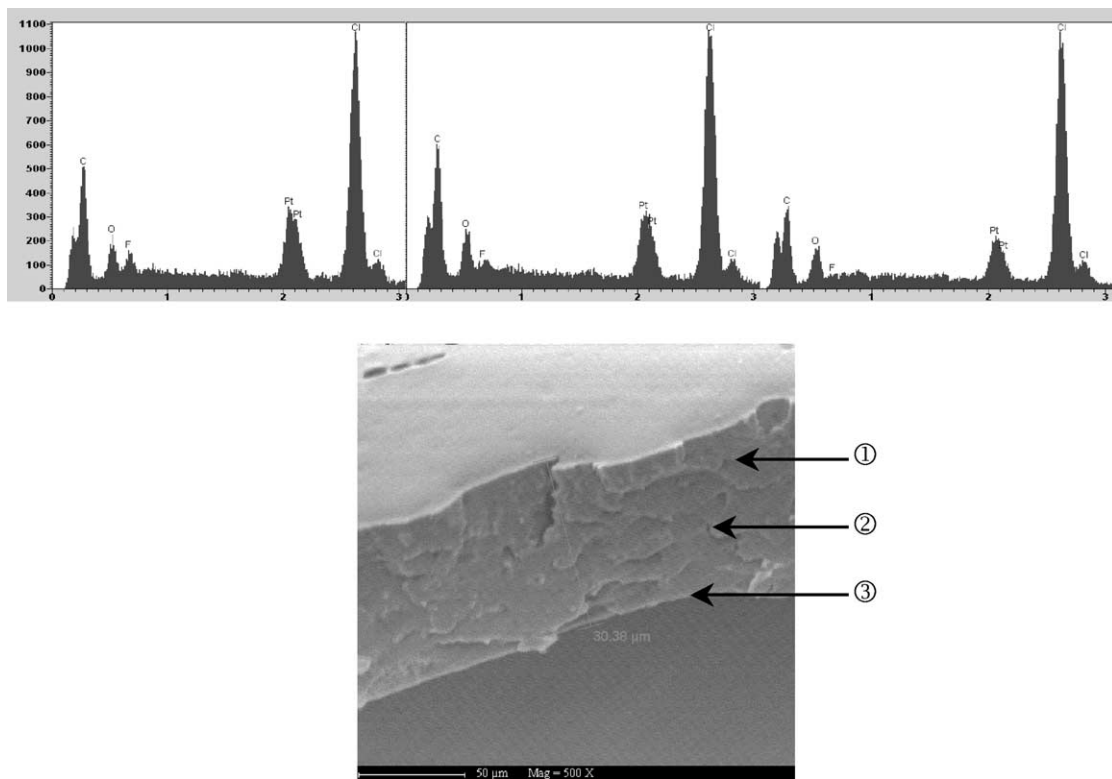


Fig. 7. EDX spectra of formulation **e** (after annealing at 110 °C): surface (left), middle of the cross section (middle), interface (right), and SEM photograph of cross section of formulation **e** (after annealing at 110 °C).



These authors showed that one of the driving forces for the ‘self-stratification’ of a polymer coating on metals is the surface energy. The additive studied herein has a rather low molecular weight so that its diffusion within the matrix is facilitated. Indeed, if the interactions between the additive and the matrix were important, leading to a complete compatibility additive/matrix, the additive would not migrate. Moreover, the incompatible moiety must contain a functionality bringing the driving force for migration. Concerning the fluorinated additive, the driving force is the difference of surface energy. This study also shows the influence of the solvent choice in order to enhance the migration: a mixture of THF and TBT permits to obtain a coating with a very low surface energy.

## References

- [1] Funke W. *J Oil Colour Chem Assoc* 1976;59:398.
- [2] Murase H, Funke W. *FATIEPEC Congress*, 15th, p. II-387–II-409; 1980.
- [3] Toussaint A. *Prog Org Coat* 1996;28:183–96.
- [4] Vink P, Bots TL. *Prog Org Coat* 1996;28:173–81.
- [5] Hansen CM. *The three dimension solubility parameter and solvent diffusion coefficient; their importance in surface coating formulation*. Copenhagen: Danisch Technical Press; 1967.
- [6] Carr C, Wallstoem E. *Prog Org Coat* 1996;28:161–71.
- [7] Benjamin S, Carr C, Walbridge DJ. *Prog Org Coat* 1996;28:197–207.
- [8] Walbridge DJ. *Prog Org Coat* 1996;28:155–9.
- [9] Hopken J, Moller M. *Macromolecules* 1992;25:2482–9.
- [10] Shimizu T. *Modern fluoropolymers*: New York: Wiley; 1997.
- [11] Sivaniah E, Genzer J, Fredrickson GH, Kramer EJ, Xiang M, Li X, et al. *Langmuir* 2001;17:4342–6.
- [12] Nagai K, Tanaka S, Hirata Y, Nakagawa T, Arnold ME, Freeman BD, et al. *Polymer* 2001;42:09941–09948.
- [13] Hikita M, Tanaka K, Nakamura T, Kajiyama T, Takahara A. *Langmuir* 2004;20:5304–10.
- [14] Lacroix-Desmazes P, Andre P, Desimone JM, Ruzette A-V, Boutevin B. *J Polym Sci, Part A: Polym Chem* 2004;42:3537–52.
- [15] Ming W, Melis F, van de Grampel RD, van Ravenstein L, Tian M, van der Linde R. *Prog Org Coat* 2003;48:316–21.
- [16] McCloskey CB, Yip CM, Santerre JP. *Macromolecules* 2002;35:924–33.
- [17] Yu Z, Zhang Z, Yuan Q, Ying S. *Adv Polym Tech* 2002;21:268–74.
- [18] Bongiovanni R, Beamson G, Mamo A, Priola A, Recca A, Tonelli C. *Polymer* 1999;41:409–14.
- [19] Tang YW, Santerre JP, Labow RS, Taylor DG. *J Appl Polym Sci* 1996;62:1133–45.
- [20] Walz SM, Malner TE, Mueller U, Muelhaupt R. *J Polym Sci, Part B: Polym Phys* 2003;41:360–7.
- [21] Matyjaszewski K, editor. *Advances in controlled/living radical polymerization*. ACS symposium held in Boston, Massachusetts 17–22 August 2002. ACS symposium series, vol. 854.
- [22] Lacroix-Desmazes P, Ameduri B, Boutevin B. *Collect Czech Chem Commun* 2002;67:1383–415.
- [23] Bicerano J, Burmester AF, DeLassus PT, Wessling RA. *Barrier polymers and structures*. Washington, DC: American Chemical Society; 1990.
- [24] Koros WJ. *Barrier polymers and structures*. Washington, DC: American Chemical Society; 1990.
- [25] Lacroix Desmazes P, Severac R, Boutevin B. *ACS Symp Ser* 2003; 854:570–85.
- [26] Severac R, Lacroix-Desmazes P, Boutevin B. *Polym Int* 2002;51:1117–22.
- [27] Chiefari J, Chong YK, Ercole F, Krstina J, Jeffery J, Le TPT, et al. *Macromolecules* 1998;31:5559–62.
- [28] Collins S, Yoda K, Anazawa N, Birkinshaw C. *Polym Degrad Stab* 1999;66:87–94.
- [29] Pittman AG. *Fluoropolymer*: Wiley Interscience; 1972.
- [30] Young T. *Proc R Soc London* 1804;95:65.
- [31] Fowkes FM. *Ind Eng Chem* 1964;56:40.
- [32] Kaelble DH. *J Adhes* 1970;2:66–81.
- [33] Owens DK, Wendt RC. *J Appl Polym Sci* 1969;13:1741–7.
- [34] Wu S. In: Wu S, editor. *Polymer interface and adhesion*. New York: Marcel Dekker; 1982. pp. 169–214. [ISBN 0-8247-1533-0].
- [35] Van Oss CJ, Good RJ, Chaudhury MK. *Langmuir* 1988;4:884–91.
- [36] Bes L, Rousseau A, Boutevin B, Mercier R, Kerboua R. *Macromol Chem Phys* 2001;202:2954–61.
- [37] Ellison AH, Zisman WA. *J Phys Chem* 1954;58:260.
- [38] Corpart JM, Girault S, Juhué D. *Langmuir* 2001;17:7237–44.